CIVIL ENGINEERING STUDIES
Illinois Center for Transportation Series No. 23-005
UILU-ENG-2023-2005
ISSN: 0197-9191

Optimal Approach for Addressing Reinforcement Corrosion for Concrete Bridge Decks in Illinois—Phase II

Prepared By
Matthew J. Gombeda
Zoe N. Lallas
Estevan Rivera Jr.
Illinois Institute of Technology

Research Report No. FHWA-ICT-23-004

A report of the findings of

ICT PROJECT R27-SP52
Optimal Approach for Addressing Reinforcement Corrosion for Concrete Bridge Decks in Illinois—Phase II

https://doi.org/10.36501/0197-9191/23-005

Illinois Center for Transportation

May 2023

TECHNICAL REPORT DOCUMENTATION PAGE

1. Report No. FHWA-ICT-23-004	**2. Government Accession No.** N/A	**3. Recipient's Catalog No.** N/A
4. Title and Subtitle Optimal Approach for Addressing Reinforcement Corrosion for Concrete Bridge Decks in Illinois—Phase II		**5. Report Date** May 2023 **6. Performing Organization Code** N/A
7. Authors Matthew J. Gombeda, Zoe N. Lallas, Estevan Rivera Jr		**8. Performing Organization Report No.** ICT-23-005 UILU-2023-2005
9. Performing Organization Name and Address Illinois Center for Transportation Department of Civil and Environmental Engineering University of Illinois at Urbana-Champaign 205 North Mathews Avenue, MC-250 Urbana, IL 61801		**10. Work Unit No.** N/A **11. Contract or Grant No.** R27-SP52
12. Sponsoring Agency Name and Address Illinois Department of Transportation (SPR) Bureau of Research 126 East Ash Street Springfield, IL 62704		**13. Type of Report and Period Covered** Final Report 5/16/22–5/15/23 **14. Sponsoring Agency Code**

15. Supplementary Notes
Conducted in cooperation with the U.S. Department of Transportation, Federal Highway Administration.
https://doi.org/10.36501/0197-9191/23-005

16. Abstract
This report presents the expansion of a previously introduced life-cycle cost calculation framework for concrete bridge decks in Illinois. In addition to the alternative reinforcement options examined in the Illinois Center for Transportation and Illinois Department of Transportation project R27-SP49, two additional reinforcing bar types—stainless steel–clad carbon core and textured epoxy-coated bars—are the main subjects of this study. The results of a comprehensive literature review of these two additional bar options will highlight their cost-benefit characteristics toward optimizing the life span of a concrete bridge deck, most notably trade-offs between often increased upfront material costs and enhanced durability over a design 100-year service life. Additionally, the scope of this study includes the development of a more robust methodology to account for the effect of the relatively high nominal yield strength and corresponding reduced ductility of A1035 bars, one of the alternate reinforcement options examined in R27-SP49. The researchers used a numerical moment-curvature-based analysis methodology to facilitate the development of a design-friendly modified high-strength reinforcement factor that supersedes the nominal yield strength factor proposed in the original version of the life-cycle cost framework. The outcomes of this project and R27-SP49 will collectively expand upon and aim to enhance the effectiveness of the originally proposed life-cycle cost framework. The outcomes will be demonstrated by presenting updated life-cycle costs and via a parametric study of two hypothetical bridge deck examples, each falling into significantly different categories for traffic demands and select performance expectations.

17. Key Words Reinforcement, Reinforced Concrete, Corrosion, Bridge Decks, Life-Cycle Analysis, A1035 Reinforcement	**18. Distribution Statement** No restrictions. This document is available through the National Technical Information Service, Springfield, VA 22161.

19. Security Classif. (of this report) Unclassified	**20. Security Classif. (of this page)** Unclassified	**21. No. of Pages** 25 + appendix	**22. Price** N/A

Form DOT F 1700.7 (8-72) **Reproduction of completed page authorized**

ACKNOWLEDGMENT, DISCLAIMER, MANUFACTURERS' NAMES

This publication is based on the results of **ICT-R27-SP52: Optimal Approach for Addressing Reinforcement Corrosion for Concrete Bridge Decks in Illinois—Phase II**. ICT-R27-SP52 was conducted in cooperation with the Illinois Center for Transportation; the Illinois Department of Transportation; and the U.S. Department of Transportation, Federal Highway Administration.

Members of the Technical Review Panel (TRP) were the following:

- Curt Evoy, TRP Chair, Illinois Department of Transportation
- Del Reeves, TRP Co-Chair, Illinois Department of Transportation
- Spencer Gibbs, Illinois Department of Transportation
- Nick Lombardi, Federal Highway Administration
- Sheila Moynihan, Illinois Department of Transportation
- Jayme Schiff, Illinois Department of Transportation
- Megan Swanson, Illinois Department of Transportation
- Dan Tobias, Illinois Department of Transportation
- Luke Wylde, Illinois Department of Transportation

EXECUTIVE SUMMARY

As discussed in the final report for Illinois Center for Transportation and Illinois Department of Transportation project R27-SP49, corrosion of reinforcement remains a major concern toward ensuring long-term durability of concrete bridges exposed to potentially harmful deterioration agents, such as deicing salts or other chloride-based chemical solutions. Several strategies exist for mitigating corrosion damage that can generally be categorized into two main categories. The first category involves enhancing the permeability characteristics of concrete to slow or restrict the migration of harmful chemicals through the pores of the concrete, thus preventing or limiting contact with the surface of the reinforcing steel, where the corrosion process initiates. Because this strategy is highly dependent on concrete's properties, it was not directly included within the scope of this study or the previous study (R27-SP49). The second category focuses on protecting the embedded reinforcing steel (or at least its surface) to prevent or limit the corrosion reaction if harmful chemicals were to permeate through the surrounding concrete. This category can be further partitioned into two sub-categories: 1) fabricating the bar out of a corrosion-resistant steel or 2) placing a non-metallic coating over the surface of a conventional black bar to inhibit the corrosion reaction. Expanding upon the database established in R27-SP49, two additional corrosion-resistant options (one falls into each of the two aforementioned sub-categories) are the main subjects of this study. Stainless steel–clad carbon core bars are manufactured with a protective stainless-steel coating that is fused to an underlying carbon steel core whereas textured epoxy-coated bars have a protective, rough coating applied to an underlying black bar. A1035 reinforcement was an option examined in the final report for R27-SP49 and was re-examined herein to further assess the implications of its relatively low ductility, despite its relatively high nominal yield strength, when estimating life-cycle costs for concrete bridge decks in Illinois.

There were two main objectives for this project. The first objective was to expand the scope of the life-cycle cost calculation framework developed as part of R27-SP49 to include both stainless steel–clad carbon core and textured epoxy-coated bars as corrosion-resistant alternatives. The second objective was to further assess the structural performance of concrete bridge decks constructed with A1035 bars as a function of both their increased yield strength and compensating for reduced ductility.

As mentioned in the final report for R27-SP49, an optimal life-cycle cost framework was designed for use by practicing bridge engineers working on Illinois Department of Transportation projects. The framework allows IDOT to recommend optimal design solutions for applications where enhanced corrosion resistance is desired and to assist IDOT officials with critical decision-making with respect to balancing life-cycle performance and life-cycle costs.

REPORT OUTLINE

This report contains five chapters, and specific details regarding each chapter are provided below.

Chapter 1 includes a brief review of the outcomes of the first phase of the study—ICT-IDOT project R27-SP49. This introduction is followed by an overview of the additional corrosion-resistant reinforcement types (and their respective characteristics and performance attributes) examined in this second phase study: stainless steel–clad carbon core and textured epoxy-coated bars. Additionally, background information on the relationship between relatively high nominal yield strength and corresponding ductility for A1035 reinforcement is presented in preparation for closer examinations of the impact of such behavior when calculating life-cycle costs.

Chapter 2 presents the outcomes of a comprehensive literature review focused on corrosion cost-benefit performance of stainless steel–clad carbon core and textured epoxy-coated bars. Also included in this chapter are discussions of life-cycle cost implications and case studies of other departments of transportation using these alternative reinforcement options for concrete bridge structures.

Chapter 3 presents the development of a more robust procedure to incorporate the mechanical properties of A1035 reinforcing bars into the larger framework to select the optimal reinforcement solution. More specifically, this chapter will examine how to assess the relative strength and ductility of a bridge deck cross-section constructed with high-strength A1035 bars relative to an equivalent version that uses conventional Grade 60 bars. This chapter will also discuss the derivation of a modified factor for high-strength reinforcement (for use in the life-cycle cost calculation framework) that compensates for reinforcement ductility in addition to nominal yield strength as originally implemented in the final report for R27-SP49.

Chapter 4 integrates the cost-benefit outcomes for the stainless steel–clad carbon core and textured epoxy-coated bars (see Chapter 2) as well as the modified high-strength reinforcement factor (see Chapter 3) into the life-cycle cost framework originally developed as part of R27-SP49. Recall that the methodology allows the user to estimate life-cycle costs for a given bridge deck considering the type of reinforcement and other applicable factors, such as structural performance limitations, location of the bridge, and cost of initial construction, among others.

Chapter 5 summarizes the findings and conclusions of this project.

TABLE OF CONTENTS

LIST OF FIGURES

LIST OF TABLES

CHAPTER 1: INTRODUCTION

BACKGROUND OF PROJECT R27-SP49

Illinois Center for Transportation and Illinois Department of Transportation project R27-SP49 (Gombeda et al., 2022) focused on the development of an optimal approach framework for determining the ideal corrosion-resistant reinforcement solution for a given concrete bridge deck in Illinois. This framework incorporated pertinent factors affecting both economic decisions and holistic performance of the bridge deck, including initial material costs, intended life cycle of the structure, recommended maintenance cycles for each bar type, location of the bridge, weather exposure category and corresponding intensity of road salt distribution, and nominal yield strength of the bars to account for any cost savings when using high-strength reinforcement with enhanced corrosion performance. Types of reinforcement examined included conventional black bars (as the control), epoxy-coated bars (currently the most widely used option for reinforced concrete structures by IDOT), two variants of galvanized bars, stainless-steel bars, and A1035 reinforcement. The framework developed in R27-SP49 demonstrated that, depending upon the specific properties and design objectives for a given bridge deck, potential cost savings and performance enhancements were achievable when selecting bars with enhanced corrosion-resistant properties despite slightly higher initial costs in some cases.

OVERVIEW OF ADDITIONAL CORROSION-RESISTANT REINFORCEMENT OPTIONS

As an expansion of the original study conducted as part of R27-SP49, two additional bar types were added to the scope of the overall study as part of this report: stainless steel–clad carbon core and textured epoxy-coated bars. The remainder of this chapter examines the fundamental properties of each reinforcement option, as highlighted in the following subsections. A brief review of structural design implications for A1035 reinforcement is also included. Chapter 2 discusses more details pertaining to specific outcomes of previous research studies that evaluated corrosion performance and corresponding life-cycle implications.

Stainless Steel–Clad Carbon Core Bars

Stainless steel–clad carbon core (SS-CCC) bars are produced by fusing an outer stainless-steel cladding to a carbon steel core via a metallurgical bond (NX Infrastructure, 2018). This method of fabrication is meant to enhance the corrosion resistance of the reinforcement by providing a more durable cladding while maintaining competitive life-cycle costs (relative to a conventional solid stainless-steel bar) due to the relatively lower costing carbon core. AASHTO M 329M/M 329-11 (AASHTO, 2019) specifies chemical requirements for both the cladding and core materials. More specifically, the carbon content of the core is limited to a maximum 0.45% by weight, with additional limitations for manganese, phosphorus, sulfur, and silicon. The requirements for the stainless-steel cladding are more numerous, starting with meeting ASTM A959 (ASTM International, 2019) prior to fusion with the carbon core. The cladding is applied to the core material prior to rolling as the completed bar is then hot rolled as a composite unit. The finished bar must have 90% of all recorded cladding thickness measurements greater than or equal to 175 µm (0.007 in.) with an absolute

minimum measurement of 125 µm (0.005 in.). The minimum bond strength between the cladding and core materials shall be 137.9 MPa (20 ksi) in accordance with ASTM A264-12 (ASTM International, 2019). AASHTO M 329M/M 329-11 also specifies minimum requirements for tensile strength and corresponding elongations. Three minimum nominal yield strengths of 300 MPa (40 ksi), 420 MPa (60 ksi), and 520 MPa (75 ksi) are permitted—designated as Grade 300 (40), Grade 420 (60), and Grade 520 (75), respectively. Corresponding minimum (ultimate) tensile strengths are specified as 482.6 MPa (70 ksi), 620.5 MPa (90 ksi), and 689.4 MPa (100 ksi), respectively. As with similar ASTM standards, minimum elongation (in 20.3 cm [8 in.] gage length) is dependent on bar size and material grade. Grade 300 (40) bars are only fabricated in bar sizes (US Customary) 3 through 6, while Grade 520 (75) bars are only furnished in bar sizes (US Customary) 11, 14, and 18. Lastly, AASHTO M 329M/M 329-11 mandates that the bar shall be free of detrimental surface imperfections—slight imperfections such as minor seams, surface irregularities, or mill scale do not necessarily require rejection of the finished bar as long as they are not expected to facilitate improper performance of the cladding.

Textured Epoxy-Coated Bars

Textured epoxy-coated (TEC) bars are produced using a proprietary, two-step process where a conventional epoxy coating is applied to a black bar followed by the textured coating (Kim & Andrawes, 2018). The underlying steel must therefore meet its corresponding ASTM standard (e.g., ASTM 706 for low-alloy steel reinforcement, etc.) prior to any additional processing. Following the completed application of the textured powder, the maximum surface roughness of the textured bars is typically greater than that of corresponding conventional epoxy-coated bars and thus is likely to facilitate improved bond performance when embedded in concrete. Although the mechanical bond performance was of significant interest when developing the textured bar, the corrosion performance must also be understood in the context of determining its effectiveness in life-cycle cost analyses—as will be done later in this report.

Life-Cycle Cost Implications of High-Strength A1035 Reinforcement

Reinforcement meeting ASTM A1035 (ASTM International, 2020) was included in the scope of R27-SP49; however, quantifying the effect of its inherently higher nominal yield strength was limited to using a nominal yield strength factor—taken as simply the ratio of 420 MPa (60 ksi) to the nominal yield strength of the A1035 bars. Although this approach captured the potential for enhanced life-cycle costs due to using lower quantities of high-strength steel, more comprehensive examinations of the influence of mechanical and structural performance on life-cycle considerations was still needed. Most notably, the constitutive properties of high-strength A1035 reinforcement exhibit relatively lower ductility compared to Grade 420 (60) reinforcing steels. This phase two study sought to examine what limited ductility would mean for structural safety of the bridge decks in the context of life-cycle cost calculations. The outcomes resulting from this objective will be detailed later in this report.

CHAPTER 2: CURRENT UNDERSTANDING OF REINFORCEMENT CORROSION PERFORMANCE IN BRIDGE DECKS

This chapter presents the results of a comprehensive literature review that focused on assessing the corrosion performance and life-cycle cost implications for stainless steel–clad carbon core and textured epoxy-coated bars, specifically for concrete bridge decks.

STAINLESS STEEL–CLAD CARBON CORE BARS

Stainless steel–clad carbon core bars are currently not used as widely as regular epoxy-coated bars but are the subject of ongoing research efforts due to their relative cost savings and similar performance in comparison to traditional stainless-steel bars. More specifically, the ability to implement a lower cost option of carbon steel with a cladding cover of stainless steel while still maintaining the corrosion-resistance properties of stainless-steel reinforcement is enticing for many departments of transportation (DOTs). Manufacturing concerns such as gaps, crevices, or unevenness in cladding often deter this type of reinforcement from being designed or constructed in concrete bridge decks from several DOTs (Tanks & Sharp, 2015). The previously mentioned provisions in AASHTO M 329M/M 329-11 that require a minimum recorded thickness of cladding on the completed bar were developed to address these concerns.

While SS-CCC bars are nearly twice the initial cost of epoxy-coated bars, they can facilitate lower life-cycle costs relative to regular epoxy-coated bars (Kahl, 2012). SS-CCC bars are currently believed to have a service life span of over 100 years with little to no repairs required due to corrosion (NX Infrastructure, 2018). SS-CCC bars also have the potential to reduce overall costs via reduced concrete cover and, in some cases, require less reinforcement to offset upfront construction cost increases (Kahl, 2012). The stainless-steel cladding reduces any damages or nicks that are often a concern associated with the handling and transportation of epoxy-coated bars. SS-CCC bars are currently permitted and used in Virginia, New York, Michigan, Oregon, and Florida DOTs. Michigan DOT has begun to overlook the 2%–8% increase in the initial cost of using SS-CCC compared to epoxy-coated bars due to projected cost savings resulting from less frequent maintenance demands for concrete bridge decks.

SS-CCC bars were used on a New York Thruway Authority Route 980D replacement bridge project because of its enhanced corrosion resistance relative to conventional black and regular epoxy-coated bars, reduced costs in comparison to traditional stainless-steel bars, and its nearly 100-year life span that satisfies the Federal Highway Administration guidelines for 75-year minimum design criteria for corrosion resistance and 75-year minimum life span (NX Infrastructure, 2018). While this bar type does exhibit higher corrosion resistance, a major risk is the end caps which, similarly to a damaged coating in epoxy-coated bars acting as an accelerated pathway for corrosion, may led to premature deterioration of the bar. To address this concern, many SS-CCC vendors cap the cut ends of the bar with a plastic sealant to protect the carbon core.

A trial bridge study by Virginia DOT showed that SS-CCC bars have mechanical properties similar to traditional solid stainless-steel bars and generally do not warrant any significant new design

limitations (Clemeña et al., 2003). Furthermore, the Virginia DOT project examined the behavior of cladding manufactured with five stainless-steel grades: 304, 304L, 316, 316L austenitic, and 2205 duplex. This study demonstrated that SS-CCC lasted 15 times longer than galvanized steel and 16 times longer than epoxy-coated bars over the same design life cycle.

TEXTURED EPOXY-COATED BARS

Since TEC is a relatively new reinforcement type with ongoing research sponsored by IDOT, most studies are pursuing lab tests that are meant to be representative of TEC installed in concrete bridge decks; however, IDOT has installed TEC bars in several concrete bridge decks. TEC has a higher initial slip resistance than regular epoxy-coated bars but also demonstrates a higher resistance to crack widening (Andrawes et al., 2022). While this initial performance is noteworthy, Kim and Andrawes (2018) observed in a separate study that once the friction resistance was surpassed, the slip resistance reduced significantly at a rapid rate. Once this slip threshold is reached, localized areas of reinforcement became exposed and would be a direct path for corrosion. The immediate drop in slip resistance, after the friction resistance was surpassed, is so drastic that it can resemble the performance of conventional, uncoated black bars. Furthermore, this drastic decrease in slip resistance can also facilitate approximately 17% reductions in peak (concrete) bond stress when compared to that of regular epoxy-coated reinforcement (Murphy, 2021).

Another corrosion-resistant performance characteristic of TEC is that when placed under temperature simulation tests, TEC can result in reduced concrete cracking by 33% relative to regular epoxy-coated bars (Andrawes et al., 2022). For a concrete bridge deck, this conclusion would mean fewer pathways for harmful deterioration agents and, thus, should facilitate an overall reduction in corrosion exposure (Andrawes et al., 2022). Peterman (2009) performed a sustained four-point bending test to determine the displacement and corresponding average crack properties of concrete specimens fabricated with TEC as well as conventional uncoated black, regular epoxy-coated, and galvanized bars. The results of that study and additional series of tests by other researchers further highlighted that TEC performs similarly to galvanized reinforcing bars with relatively smaller average crack properties when compared to uncoated black bars and regular epoxy-coated reinforcement (Murphy, 2021).

NOTE ON ASTM A1035 BARS

Although structural performance considerations for A1035 bars are a major focus of this report, a detailed summary of the corrosion performance of this reinforcement type can be found in the final report for R27-SP49 (Gombeda et al., 2022).

CHAPTER 3: EXAMINATION OF A1035 REINFORCEMENT DUCTILITY AND IMPLICATIONS FOR LIFE-CYCLE ANALYSIS

The final report of R27-SP49 (Gombeda et al., 2022) presented a "nominal yield strength factor" to estimate the advantages to life-cycle cost calculations when utilizing high-strength reinforcement (i.e., with a nominal yield strength greater than 414 MPa [60 ksi] for the purposes of that and this study). The factor was simply calculated as the quotient of 414 MPa (60 ksi) (as the conventional nominal yield strength) and the nominal yield strength of the high-strength reinforcement of interest. As an example, using A1035 bars with a minimum nominal yield strength of 689 MPa (100 ksi) would theoretically reduce life-cycle costs after multiplying by a factor of 0.6. A shortcoming of this approach is the absence of a metric for reduced ductility that often accompanies higher strength reinforcing steels. In certain cases, reduced ductility may limit design flexibility for concrete bridge decks, as higher ductility performance generally facilitates enhanced structural safety via more gradual failure mechanisms that are numerically represented in design practice by more liberal strength-reduction factors. The development of a modified high-strength reinforcement factor presented herein aims to account for expected ductility in the life-cycle assessment framework and therefore provide a more robust estimate of its effect when calculating life-cycle costs.

THEORY OF NUMERICAL MODEL

The model used to assess concrete bridge deck ductility for the purposes of this report is fundamentally based on the moment-curvature relationship for a given reinforced concrete cross-section. Curvature, ϕ, quantifies the degree of bending within a cross-section and, more specifically, directly relates the strain in the extreme compression fiber of the section, ε_c, to the neutral axis depth, c, as shown in Figure 1.

$$\varphi = \tan^{-1}\left(\frac{\varepsilon_c}{c}\right)$$

Figure 1. Equation. Calculation of curvature, φ.

Moment-curvature relationships have been used extensively to assess the performance of reinforced concrete structures, especially when ductility is of particular importance. Generally, ductility is defined as the ratio of the ultimate deformation capacity of a structural member relative to its yield deformation. (Users can substitute curvature for deformation when examining solely the cross-section, as will be done in this report.) Therefore, larger ductility values tend to correspond to structures that are able to continue accruing load or deformation, or both, past initial yielding or plastic hinge formation and are less likely to exhibit catastrophic failure modes without warning. In the context of this study, moment-curvature relationships will be used to assess the relative ductility of a concrete bridge deck with high-strength A1035 reinforcement compared to that of a bridge deck section where conventional Grade 60 reinforcement is used—with all other design parameters held constant.

The approach to calculate the relationship between the curvature of the cross-section and the corresponding moment resistance in this study is based on a fiber cross-section model. Using this method, a reinforced concrete cross-section is first partitioned into discrete fibers (or layers) that are "cut" parallel to the axis which the moment resistance is evaluated about. Each fiber is loaded solely as an axial element, and a strain, stress, and resultant force value is computed at its geometric centroid. The strain value is calculated using the assumption of strain compatibility for a given value of ε_c and the corresponding value of c that achieves cross-sectional equilibrium (i.e., the net sum of all resultant forces across all fibers on the cross-section is approximately zero). The stress in each fiber is computed using the strain at that location to interpolate on the constitutive stress-strain material relationship for either concrete or the type of reinforcement used, depending on what materials that particular fiber is comprised of. The resultant force is then computed as the product of the fiber stress and the area of the individual fiber partition. Once equilibrium is achieved (and thus the correct value of c is determined) for a given value of ε_c, curvature is computed using the equation shown in Figure 1 and the corresponding moment resistance is calculated as the sum of each fiber's individual moment contribution (i.e., the product of the fiber's resultant force and the distance from its centroid to the reference point on the cross-section). This procedure is then repeated for increasingly larger values of ε_c to develop the complete moment-curvature relationship curve with which ductility can be assessed. This curve can also be used to compute the deflection of a structural member containing the cross-section properties used to generate the moment-curvature relationship. Specific details on the calculation of deflections using moment-curvature analysis can be found in a previous publication by one of the authors (Gombeda et al., 2017).

VALIDATION OF NUMERICAL MODEL

Because moment-curvature analysis will be the primary method for assessment of ductility in this report, the numerical model used to develop such relationships must first be validated against experimental test data. It is difficult to measure curvature during a physical test, so the validation scheme used herein will be based on moment-deflection relationships. The theoretical moment-deflection curve will be based on the moment-curvature approach described previously, while experimental results were obtained from a series of previous experimental tests on reinforced concrete panels conducted by one of the authors (Gombeda et al., 2019). More specifically, three variants of a solid reinforced concrete wall panel were tested to failure in flexure—during which both the moment resistance and corresponding deformation were recorded. Please note that for the purposes of this report, the deformation response is presented as support rotation, which essentially normalizes the midspan deformation of the member to one-half of the span length. The design details of the three panel variants—ET025, ET015, and ET005—can be found in Gombeda et al. (2019), where each variant has an identical gross cross-section geometry but varying reinforcement ratios. Specimen type ET005 was designed to exhibit approximately one-third and one-fifth the ductility of specimen types ET015 and ET025, respectively. Therefore, using this particular set of experimental data is appropriate for this study, in which examination of relative ductility is a primary objective.

Figures 2, 3, and 4 show comparisons between the moment versus support rotation relationships obtained from the theoretical model ("Model") and experimental tests from Gombeda et al. (2019) for panel types ET025, ET015, and ET005, respectively. Note that triplicate specimens were tested for ET025 and ET015, while only data for duplicate members were available for ET005. The "Model" curve for each variant generally shows a good correlation to the experimental test data across all panel types, especially up to the approximate peak moment resistance. These results promote confidence that the moment-curvature-based theoretical model is appropriate for the purposes of this study to assess the structural performance of reinforced concrete sections with expected variations in ductility.

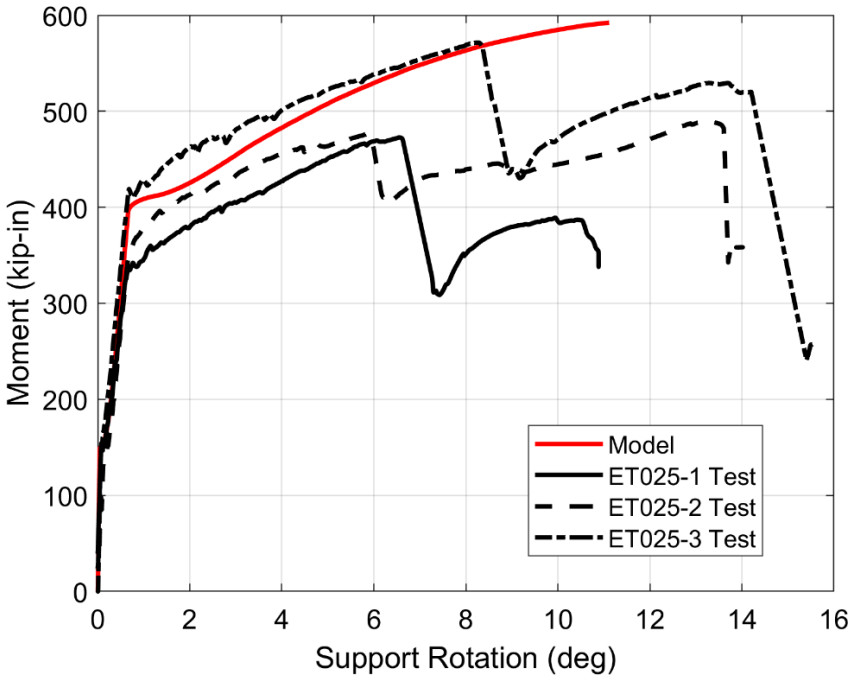

Figure 2. Graph. Comparison of experimental test data to modeling results for ET025 specimens.

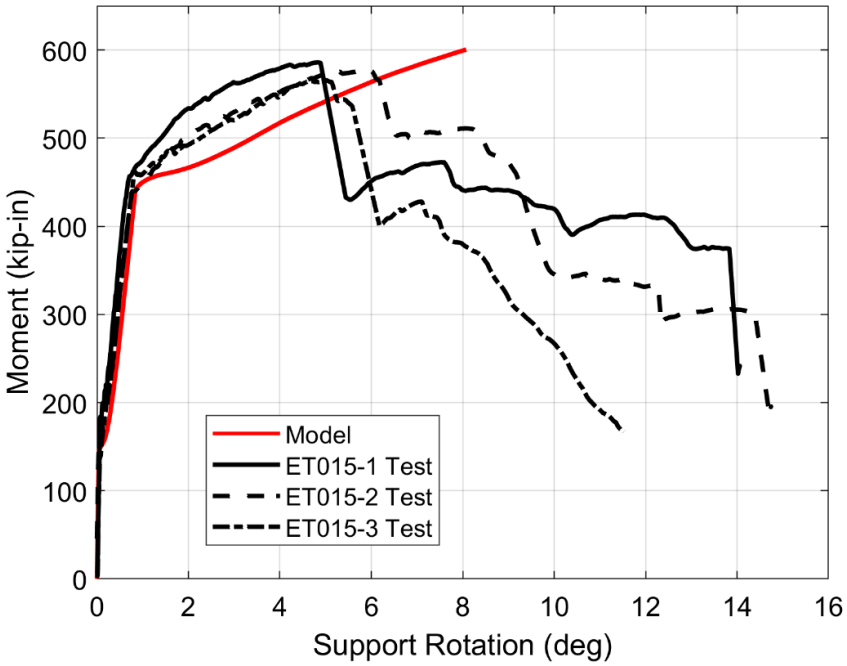

Figure 3. Graph. Comparison of experimental test data to modeling results for ET015 specimens.

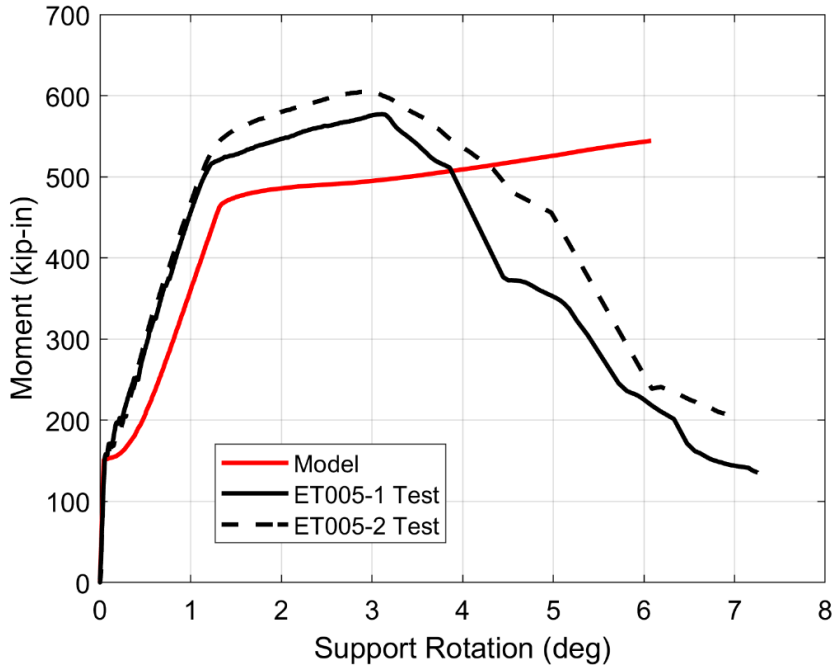

Figure 4. Graph. Comparison of experimental test data to modeling results for ET005 specimens.

PARAMETRIC STUDY OF CONCRETE BRIDGE DECK SECTIONS

After validating the theoretical model, the underlying moment-curvature approach was then utilized to conduct a comprehensive parametric study to assess ductility in concrete bridge deck sections constructed with A1035 high-strength reinforcement compared to the same concrete section constructed with conventional Grade 60 bars. Recall that many of the alternative reinforcement options examined in R27-SP49 had standard nominal yield strengths of 420 MPa (60 ksi), although the constitutive stress–strain relationships used for the conventional case herein were gathered from tensile testing of Grade 60 black bars as part of a previous research project (Gombeda et al., 2019). Trial bridge deck cross-section geometries were obtained from IDOT's *Bridge Manual* (2012) and reproduced in Figure 5, where S is the transverse span between adjacent bridge beams and ρ is the reinforcement ratio calculated using the equation in Figure 6. A unique reinforcement ratio can be calculated for each of the top (ρ_{top}) and bottom (ρ_{bot}) bar layers, where the depth to the centroid of the reinforcement, d, is taken relative to the extreme compression fiber (i.e., the top of the section in positive bending and the bottom in negative bending over the supports). Trial reinforcement ratios for the parametric study were determined using design charts in Section 3.2 of IDOT's *Bridge Manual* by interpolating the required areas of bottom and top reinforcement, A_s and A_s', respectively (which will later be converted to reinforcement ratios, ρ and ρ', respectively, using the equation shown in Figure 6). Even though compression reinforcement may be neglected in design for the purposes of calculating nominal flexural resistance by IDOT, it is included as part of the life-cycle cost calculation framework due to good correlation observed with ductility performance parameters. Please note that ρ' uses the same equation form but substitutes the area of compression reinforcement, A_s', for the area of tension reinforcement as a function of the transverse span between adjacent girders, S, and the total thickness of the deck. Additionally, the reinforcement ratios used in tension and compression were calculated pursuant to Section 3.2 of IDOT's *Bridge Manual*. Two trial span lengths of 1.83 m (6 ft) and 2.59 m (8.5 ft) were selected in combination with two trial total deck thicknesses of 19.1 cm (7.5 in.) and 20.3 cm (8 in.). A tributary width of 30.5 cm (1 ft) was used for each trial cross-section. After using the design chart in IDOT's *Bridge Manual* to determine the required top and bottom reinforcement ratios for the conventional Grade 60 bars, equivalent reinforcement ratios for two cases applicable to using A1035 bars were then calculated by solving for the required reinforcement ratio to produce an equivalent nominal flexural resistance of the Grade 60 doubly-reinforced section over the supports (i.e., in the negative bending region) when the nominal yield strength increased. The first case involved conservatively limiting the nominal yield strength of the A1035 reinforcement to 551.6 MPa (80 ksi), as is often done in design practice. The second case utilized the full nominal strength yield of 689.5 MPa (100 ksi). Note that even though the reinforcement was resized only in the negative moment region, a simplifying assumption was made that the bar layouts would be prismatic across the span of the deck. The concrete strength in all cases was taken as 27.6 MPa (4 ksi). The complete matrix of all 24 trial cross-section configurations is shown in Table 1. Note that for this set of trials the concrete compressive strength was set at 27.6 MPa (4000 psi), however, this parameter can also be modified by the user (just like the reinforcement properties and cross-section geometry) for a given scenario by following the general procedure of this framework.

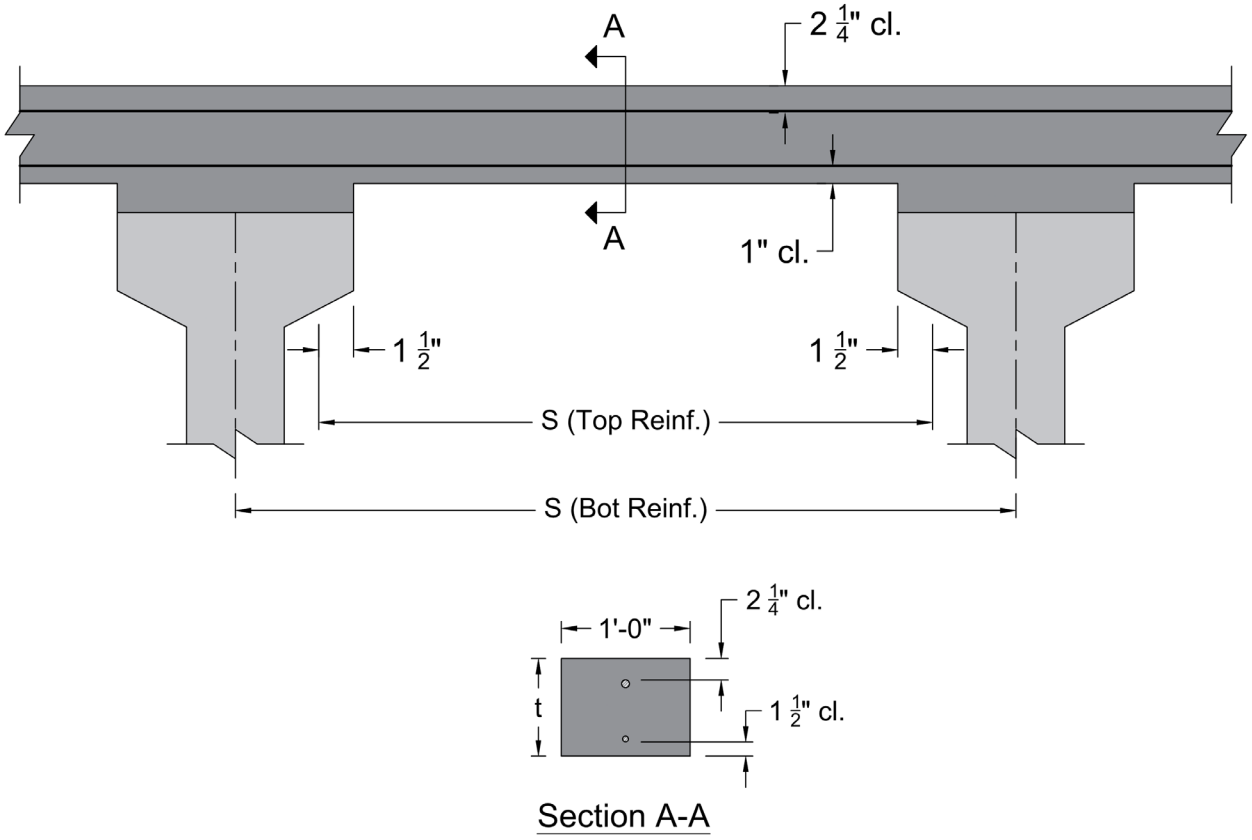

Figure 5. Illustration. Trial bridge deck section and associated parameters. An acceptable tolerance for bar placement in this case is +/- ¼".

$$\rho = \frac{A_s}{bd}$$

Figure 6. Equation. Calculation of reinforcement ratio, *ρ*.

Table 1. Matrix of Trial Concrete Bridge Deck Cross-Sections

Section ID	Trans. Span (ft)	Deck Thickness (in)	Moment Orientation	Reinf. Type	ρ	ρ'	Mn (kip-in)
S6t7.5-N60	6	7.5	Negative	fy Gr. 60	0.861%	0.624%	155.2
S6t7.5-N80				0.8*fy A1035	0.650%	0.471%	155.3
S6t7.5-N100				fy A1035	0.522%	0.378%	155.2
S6t7.5-P60			Positive	fy Gr. 60	0.542%	0.747%	158.6
S6t7.5-P80				0.8*fy A1035	0.409%	0.564%	172.4
S6t7.5-P100				fy A1035	0.328%	0.453%	170.1
S8.5t7.5-N60	8.5	7.5	Negative	fy Gr. 60	1.215%	0.861%	205.6
S8.5t7.5-N80				0.8*fy A1035	0.913%	0.646%	205.4
S8.5t7.5-N100				fy A1035	0.731%	0.518%	205.6
S8.5t7.5-P60			Positive	fy Gr. 60	0.747%	1.055%	196.0
S8.5t7.5-P80				0.8*fy A1035	0.561%	0.793%	214.8
S8.5t7.5-P100				fy A1035	0.450%	0.634%	213.1
S6t8-N60	6	8	Negative	fy Gr. 60	0.644%	0.490%	145.7
S6t8-N80				0.8*fy A1035	0.487%	0.371%	145.7
S6t8-N100				fy A1035	0.392%	0.299%	145.7
S6t8-P60			Positive	fy Gr. 60	0.431%	0.566%	144.5
S6t8-P80				0.8*fy A1035	0.326%	0.428%	155.7
S6t8-P100				fy A1035	0.263%	0.345%	153.5
S8.5t8-N60	8.5	8	Negative	fy Gr. 60	0.966%	0.705%	203.1
S8.5t8-N80				0.8*fy A1035	0.726%	0.530%	203.3
S8.5t8-N100				fy A1035	0.581%	0.425%	202.9
S8.5t8-P60			Positive	fy Gr. 60	0.620%	0.848%	183.5
S8.5t8-P80				0.8*fy A1035	0.466%	0.638%	199.9
S8.5t8-P100				fy A1035	0.373%	0.510%	197.5

ASSESSMENT OF DUCTILITY FOR BRIDGE DECKS CONTAINING A1035 BARS

Figures 7–10 present the M-φ relationships for the 24 trial cross-sections listed in Table 1. Each figure contains two subplots—one each for the negative and positive moment regions. Within each subplot are three distinct M-φ curves, one each for the conventional Grade 60, maximum 551.6 MPa (80 ksi), and full 689.5 MPa (100 ksi) layouts. An important objective when examining these figures is assessing the relative ductility between the sections constructed with conventional Grade 60 bars and those comprised of the high-strength A1035 bars. More specifically, this examination will emphasize the following key aspects related to ductility: 1) the curvature at peak moment resistance when using expected stress–strain relationships relative to the curvature corresponding to the nominal flexural resistance and 2) the remaining ductility present after the peak moment resistance is achieved up to

the point where significant moment resistance is lost in the post-peak M-φ region. The latter of the two aspects is used to arrive at a qualitative indication of design safety—demonstrating how much actual moment resistance remains after the nominal flexural resistance (listed for each section in Table 1) has been achieved. The second aspect provides a qualitative measure of how catastrophic the expected failure mode of the section would be after achieving its peak moment resistance.

Generally, Figures 7–10 demonstrate that the cross-sections examined in this study exhibit significant expected strength past their corresponding nominal flexural resistance, especially for the A1035 bars limited to 80% of their nominal yield strength (i.e., 80 ksi). This behavior is caused by requiring a larger area of reinforcement to meet a similar nominal flexural resistance when the available nominal yield strength is reduced by 20%. An identical expected stress–strain relationship was used for the 80% and 100% A1035 yield strength trials because only the design yield strength is limited—which has no effect on its expected performance. Therefore, the curvature at which significant moment resistance is lost is generally very similar between the 80% and 100% A1035 yield strength trials in this study, as indicated in Figures 7–10 by the abrupt drop-off in moment resistance. These curvatures are, however, significantly lesser in magnitude when compared to the corresponding values for the sections containing Grade 60 reinforcement. These general observations of behavior reinforce the need for a higher-fidelity factor that considers both design over-strength and relative ductility in the life-cycle cost calculation methodology.

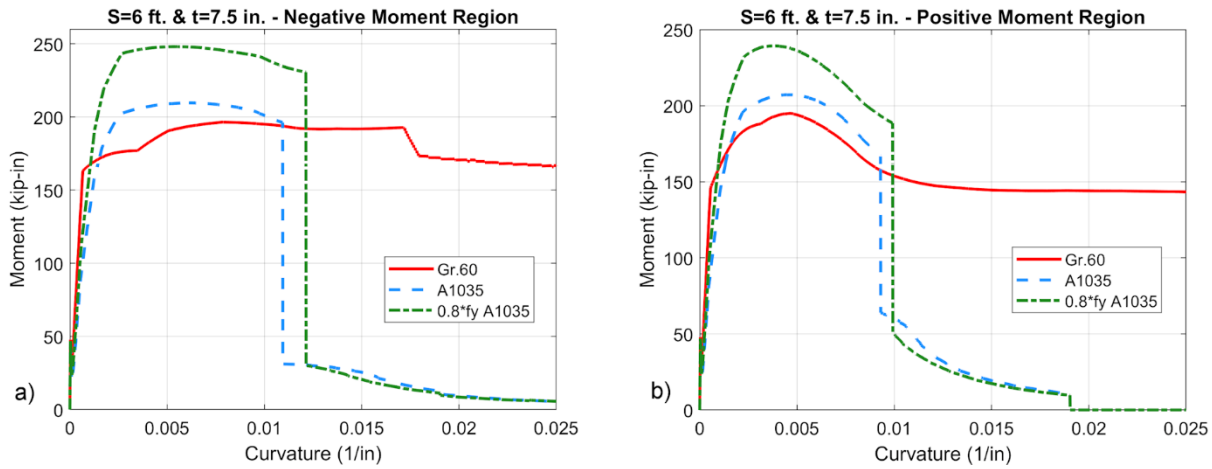

Figure 7. Charts. M-φ curves for S = 1.83 m (6 ft) and t = 19.1 cm (7.5 in).

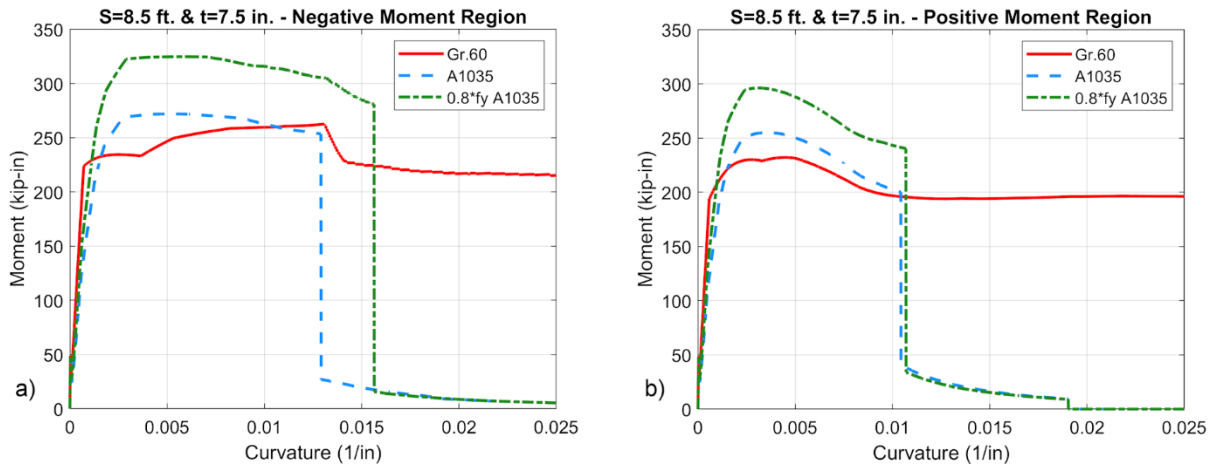

Figure 8. Charts. M-φ curves for S = 2.59 m (8.5 ft) and t = 19.1 cm (7.5 in).

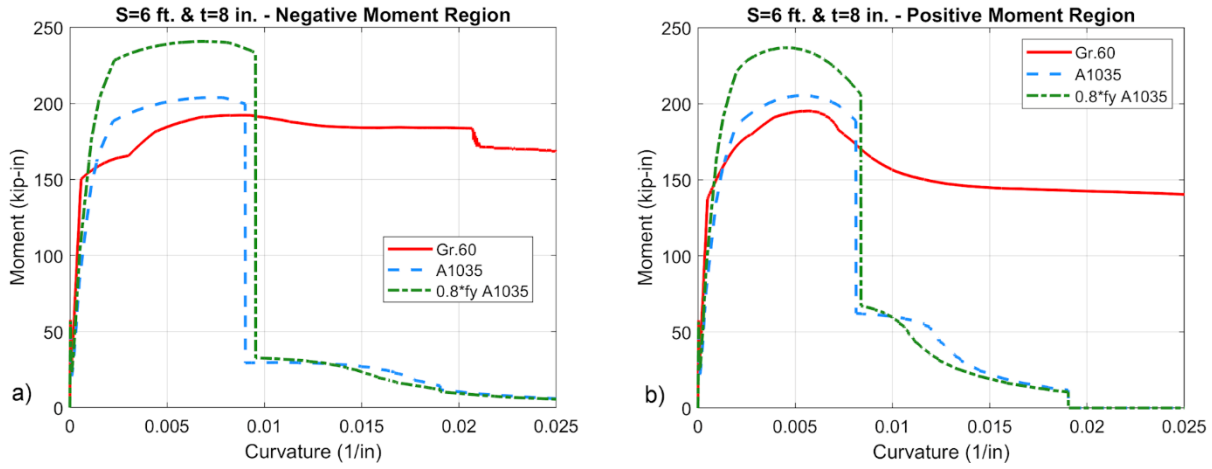

Figure 9. Charts. M-φ curves for S = 1.83 m (6 ft) and t = 20.3 cm (8 in).

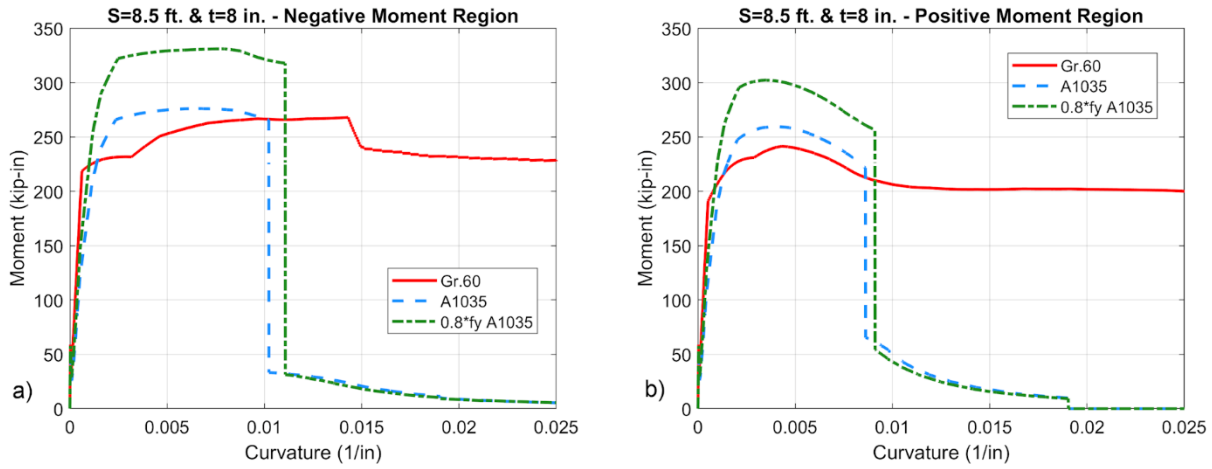

Figure 10. Charts. M-φ curves for S = 2.59 m (8.5 ft) and t = 20.3 cm (8 in).

DEVELOPMENT OF THE MODIFIED HIGH-STRENGTH REINFORCEMENT FACTOR

Because it can be difficult to perform a moment-curvature analysis during the design of a reinforced concrete bridge deck, a design-focused methodology was developed based on the results of the M-φ behavior shown in Figures 7–10. One of the main factors used to compensate for ductility in conventional reinforced concrete design is the strength-reduction factor, which is used to calculate the reduced strength level available for design as a function of the net tensile strain, ε_t, of the reinforcement and the corresponding yield strain at nominal yield strength, ε_y. Recall that ε_t is calculated at the extreme tension layer of reinforcement in the section even if multiple rows of tension reinforcement are present. The difference between ε_t and ε_y quantifies the ductility once the nominal flexural resistance is achieved. Therefore, the larger this difference qualitatively, the less likely a structure containing that cross-section would fail suddenly or catastrophically and, thus, is generally more favorable in examinations of structural safety and reliability. The development of actual strength-reduction factors generally requires comprehensive stochastic and reliability-focused analyses, which are not within the scope of this project. Therefore, a simplified approach was developed to calculate a modified high-strength reinforcement factor in lieu of calculating a strength-reduction factor. This simplified approach allows the user to input ε_t and ε_y obtained from the cross-section analysis of the bridge deck during design. The first step involves calculating the ductility factor, λ, which is the difference of ε_t and ε_y for the cross-section of interest divided by the difference of ε_t and ε_y for an equivalent cross-section containing conventional Grade 60 bars, as shown in the equation in Figure 11. The resulting ductility factor is then used to calculate the modified high-strength reinforcement factor, ψ, using the equation in Figure 12. The factor ψ is very similar in form to the nominal yield strength factor (NYSF) originally proposed in R27-SP49 (Gombeda et al., 2022) with the new addition of the ductility factor, λ, in the denominator of the equation. Increasing values of λ, which indicate greater ductility, will result in decreasing values of ψ, which, when implemented as a replacement for the original NYSF in the life-cycle cost framework, facilitate lower life-cycle costs. Conceptionally, the greatest decrease in life-cycle costs can be achieved by using a higher design yield strength (which, as discussed in R27-SP49, will lead to smaller quantities of bars required and corresponding material cost savings) that is also accompanied by relatively high ductility. For the case of A1035 bars with a higher nominal yield strength and relatively lower ductility, the new ψ factor provides a balance between the two design considerations with more robustness compared to the original NYSF factor.

$$\lambda = \frac{\varepsilon_t - \varepsilon_y}{\varepsilon_{t\_Gr60} - \varepsilon_{y\_Gr60}}$$

Figure 11. Equation. Calculation of the ductility factor, λ.

$$\psi = \frac{60\ ksi}{\lambda\ f_y}$$

Figure 12. Equation. Calculation of the modified high-strength reinforcement factor, ψ.

Table 2 shows the data used to calculate the modified high-strength reinforcement factor, ψ, for each trial cross-section section examined in the parametric study. The values of ε_t and ε_y are listed first—having been calculated when the trial cross-sections were designed. In most cases, the ductility factor, λ, decreases with increasing design yield strength, except for the S6t8-P trial sections. After calculating ψ for each case, the results in Table 2 show that this parameter decreases significantly with increasing design yield strength, as expected. The original NYSF factor proposed in R27-SP49 was also included and subsequently used to normalize the new ψ values in an attempt to compare the effectiveness of the two slightly different approaches for capturing both reinforcement over-strength and, now, available ductility with the modified factor. Values of this ratio greater than one indicate a higher life-cycle cost using the new factor compared to the original, as is the case for each trial cross-section utilizing some degree of higher design yield strength. This result is the direct and quantifiable effect of compensating for reduced ductility in high-strength reinforcement. The magnitudes of these values are only slightly greater than one. This finding is qualitatively reasonable because, despite the reduced ductility of A1035 bars, significant expected moment resistance remains after achieving the corresponding nominal flexural resistance, which inherently enhances the safety of the structure.

Table 2. Data Used in the Calculation of the Modified High-Strength Reinforcement Factor, ψ

Section ID	Design ε_y (in/in)	Design ε_t (in/in)	Ductility Factor, λ	ψ	NYSF	ψ/NYSF
S6t7.5-N60	0.00207	0.01061	1.000	1.000	1	1.000
S6t7.5-N80	0.00276	0.01102	0.968	0.775	0.75	1.034
S6t7.5-N100	0.00345	0.01135	0.925	0.648	0.6	1.081
S6t7.5-P60	0.00207	0.01061	1.000	1.000	1	1.000
S6t7.5-P80	0.00276	0.01061	0.920	0.815	0.75	1.087
S6t7.5-P100	0.00345	0.01131	0.921	0.652	0.6	1.086
S8.5t7.5-N60	0.00207	0.00851	1.000	1.000	1	1.000
S8.5t7.5-N80	0.00276	0.00866	0.916	0.819	0.75	1.092
S8.5t7.5-N100	0.00345	0.00875	0.824	0.729	0.6	1.214
S8.5t7.5-P60	0.00207	0.00851	1.000	1.000	1	1.000
S8.5t7.5-P80	0.00276	0.00880	0.938	0.800	0.75	1.066
S8.5t7.5-P100	0.00345	0.00928	0.906	0.662	0.6	1.104
S6t8-N60	0.00207	0.01327	1.000	1.000	1	1.000
S6t8-N80	0.00276	0.01393	0.997	0.752	0.75	1.003
S6t8-N100	0.00345	0.01444	0.981	0.612	0.6	1.020
S6t8-P60	0.00207	0.01327	1.000	1.000	1	1.000
S6t8-P80	0.00276	0.01292	0.907	0.827	0.75	1.103
S6t8-P100	0.00345	0.01378	0.922	0.651	0.6	1.084
S8.5t8-N60	0.00207	0.01043	1.000	1.000	1	1.000
S8.5t8-N80	0.00276	0.01070	0.949	0.790	0.75	1.054
S8.5t8-N100	0.00345	0.01092	0.893	0.672	0.6	1.119
S8.5t8-P60	0.00207	0.01043	1.000	1.000	1	1.000
S8.5t8-P80	0.00276	0.01043	0.917	0.818	0.75	1.090
S8.5t8-P100	0.00345	0.01105	0.908	0.661	0.6	1.101

CHAPTER 4: APPLICATION OF EXPANDED LIFE-CYCLE COST FRAMEWORK

This chapter presents an expanded scope of the comprehensive framework for determining the optimal corrosion-resistant reinforcement option for a given concrete bridge deck (specifically detailed for bridge decks in Illinois) originally presented in the final report for ICT-IDOT project R27-SP49 (Gombeda et al., 2022). The following additions to the overall framework are largely based upon the results of Chapters 2 and 3 in this report.

REVIEW OF ORIGINAL FRAMEWORK

Comprehensive details behind the development of the original life-cycle cost framework can be found in the final report for R27-SP49 (Gombeda et al., 2022). The methodology was based on a target service life of 100 years and computed relative (i.e., normalized the costs of alternative reinforcement options to those of conventional black bars) life-cycle costs as a function of the reinforcing bar type, initial construction costs (including materials and labor), unit repair costs, and the number of repair cycles expected within the 100-year life span. Two approaches were discussed to facilitate straightforward calculation of the total life-cycle costs—a theoretical method and a simplified procedure. The former approach implemented a higher fidelity mathematical strategy that compensated for inflation whereas the latter essentially is a direct summation of the expected costs within the 100-year life span. To facilitate more robust cost estimates when necessary, an expanded framework was also proposed that allowed for inclusion of a weather factor, effects of traffic volume, type of road classification, and the aforementioned NYSF in its original form. Finally, to assess the effectiveness of the framework, life-cycle costs were calculated for two hypothetical bridge decks—each with an option for each alternative reinforcing bar type considered in that study.

MATERIAL AND REPAIR COSTS FOR TEC AND SS-CCC BARS

Table 3 summarizes the material and repair costs as well as recommended maintenance cycles within a 100-year design service life for concrete bridge decks constructed with TEC and SS-CCC bars. Note that data for conventional black bars, regular epoxy-coated bars, and stainless-steel bars (extracted from the final report for R27-SP49) are included in the table for comparison with the two new alternatives. This motivation for comparison is especially relevant for the TEC bars, as they are similar to the regular epoxy-coated bars in composition. The values in Table 3 suggest that TEC bars are also very similar to regular epoxy-coated bars in both expected initial construction costs and repair cycle over the assumed 100-year service life. TEC bars performed slightly better in terms of the duration before maintenance activities are recommended, despite a slightly higher initial cost. SS-CCC bars perform similarly in terms of maintenance cycle to conventional stainless-steel bars in that no maintenance events are recommended within the 100-year service life—albeit with significantly lower upfront costs, as shown in Table 3. This significant cost difference is expectedly due to the presence of a carbon steel core beneath the stainless cladding, thus optimizing material usage while maintaining high corrosion resistance on the surface of the bar.

Table 3. Breakdown of Calculation for Material and Repair Costs over a 100-Year Service Life

Bar Type	Initial Cost ($/0.84m²) [$/yd²]	Repair Event Number					Unit Material Repair Cost ($/0.84m²) [$/yd²]
		1	2	3	4	5	
		Time to Repair (Years)					
Black Bar*	$1.00	24.33	48.63	72.98	85.20	96.10	$1.00
Epoxy Coated*	$1.10	49.45	85.20	x	x	x	$1.06
TEC	$1.26^	56.87†	97.98†	x	x	x	$1.06
Stainless Steel*	$3.97	x	x	x	x	x	$0.00
SS-CCC	$2.60^	x^	x^	x^	x^	x^	$0.00

*Costs for these bar types were calculated in the final report for R27-SP49 (Gombeda et al., 2022).

^Adopted from Clemeña et al (2003).

†Adopted from Ross et al (2021).

Theoretical and simplified life-cycle costs are summarized in Table 4 and are graphically presented in Figure 13. Comparing TEC bars to regular epoxy-coated bars reveals that TEC bars exhibit slightly higher life-cycle costs using the theoretical approach and for both the 75- and 100-year design service lives using the simplified methodology. This discrepancy is possibly due to the long-term durability of the roughened coating which, when damaged due to bar slip in some cases, may facilitate accelerated corrosion (see Chapter 2). However, since the life-cycle costs between the two are still similar, the TEC bars may be a suitable option where a design necessitates enhanced bond strength. Because neither SS-CCC nor conventional stainless-steel bars require a maintenance event within the 100-year life span, the simplified life-cycle costs at 50, 75, and 100 years is exactly the same as the corresponding theoretical values. The total expected cost is therefore significantly lower for the SS-CCC bars due to reduced upfront costs, as previously shown in Table 3.

Table 4. Calculation of Estimated Theoretical and Simplified Life-Cycle Costs

Bar Type	Initial Cost ($/0.84m²) [$/yd²]	Material Repair Cost ($/0.84m²) [$/yd²]	Estimated Theoretical Material Life-Cycle Cost ($/0.84m²) [$/yd²]	Simplified Life-Cycle Cost		
				50-Year Life Cycle	75-Year Life Cycle	100-Year Life Cycle
Black Bar*	$1.00	$1.00	$2.57	$3.00	$4.00	$6.00
Epoxy Coated*	$1.10	$1.06	$1.69	$2.15	$2.15	$3.21
TEC	$1.26	$1.06	$1.76	$1.26	$2.32	$3.37
Stainless Steel*	$3.97	$0.00	$3.97	$3.97	$3.97	$3.97
SS-CCC	$2.60	$0.00	$2.60	$2.60	$2.60	$2.60

*Costs for these bar types were calculated in the final report for R27-SP49 (Gombeda et al., 2022).

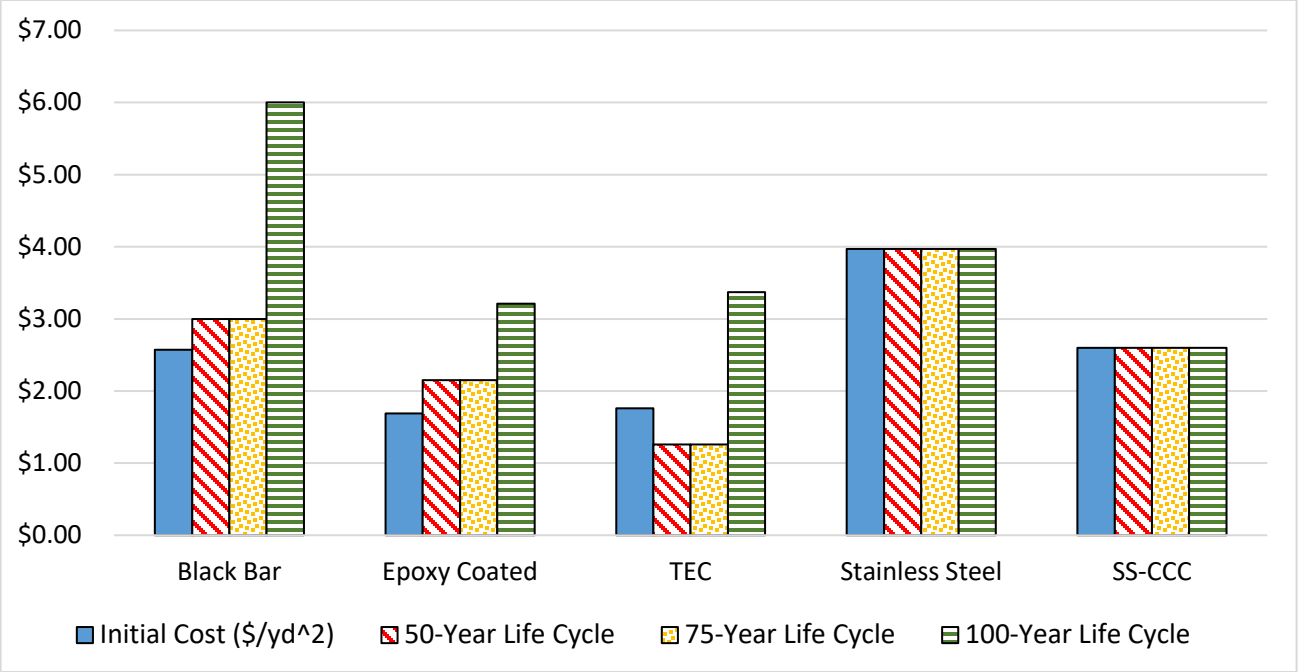

Figure 13. Chart. Graphical representation of summarized life-cycle costs.

SELECT EXAMPLES USING TEC AND SS-CCC BARS

The two hypothetical examples used in the final report for R27-SP49 will also be utilized herein to illustrate the effectiveness of the life-cycle cost framework when considering TEC and SS-CCC bars. Table 5 provides a summary of the expected life-cycle costs for the two example bridge decks in Illinois. These results are also graphically represented in Figures 14 and 15. The weather, size, and annual average daily traffic (AADT) factors are equal to those used in R27-SP49 as the example structures have not changed—other than the varying bar types. Recall that the NYSF originally proposed in R27-SP49 has been removed, and it has been replaced by a higher-fidelity approach in this report. Because the newly proposed modified high-strength reinforcement factor must be calculated for a given bridge deck—it is no longer a blanket value that strictly corresponds to the nominal yield strength of the bar—it has been excluded from Table 5. The user must remember to multiply the life-cycle costs as performed in these examples by the modified high-strength reinforcement factor before drawing any conclusions from the framework—even though A1035 bars are not listed in Table 5. The examples presented in Table 5 utilize only Grade 60 bars, and, thus, the modified high-strength reinforcement factor is one in each of those cases. It is also important to remember that it is possible to use other reinforcement types with nominal yield strengths greater than 414 MPa (60 ksi). Therefore, it is especially important to calculate the modified high-strength reinforcement factor in such cases. The results presented in Table 5 show that the regular epoxy-coated bars exhibit the lowest theoretical material life-cycle cost for both structures. The results are drastically different using the simplified life-cycle cost methodology where the TEC bars exhibit the lowest cost for a 50-year design life. Furthermore, for 75- and 100-year design lives, the SS-CCC bars are the lowest cost option—highlighting the further advantages of not needing major maintenance events within a longer design life despite relatively higher initial costs.

Table 5. Summary of Life-Cycle Costs for Two Examples

Example Selection		Simplified Life-Cycle Cost Analysis				Bar Selection Factors			Expand Life-Cycle Cost Comparison			
Example Case	Bar Type	Theoretical Material Life-Cycle Cost ($/0.84m^2) [$/yd^2]	Simplified Life-Cycle Cost			Weather Factor, WF	Bridge Size Factor, SF	AADT Factor	Theoretical Material Life-Cycle Cost^ ($/0.84m^2) [$/yd^2]	Simplified Life-Cycle Cost^		
			50 Years	75 Years	100 Years					50 Years	75 Years	100 Years
Mannheim Bridge (Lake and St. Charles), Cook County	Black Bar*	$2.57	$3.00	$4.00	$6.00	0.625	0.85	0.50	$0.68	$0.80	$1.06	$1.59
	Epoxy Coated*	$1.69	$2.15	$2.15	$3.21	0.625	0.85	0.50	$0.45	$0.57	$0.57	$0.85
	TEC	$1.76	$1.26	$2.32	$3.37	0.625	0.85	0.50	$0.47	$0.34	$0.61	$0.90
	Stainless Steel*	$3.97	$3.97	$3.97	$3.97	0.625	0.85	0.50	$1.05	$1.05	$1.05	$1.05
	SS-CCC	$2.60	$2.60	$2.60	$2.60	0.625	0.85	0.50	$0.69	$0.69	$0.69	$0.69
Rural Interstate, Southern Illinois	Black Bar*	$2.57	$3.00	$4.00	$6.00	0.375	0.65	0.25	$0.16	$0.18	$0.24	$0.37
	Epoxy Coated*	$1.69	$2.15	$2.15	$3.21	0.375	0.65	0.25	$0.10	$0.13	$0.13	$0.20
	TEC	$1.76	$1.26	$2.32	$3.37	0.375	0.65	0.25	$0.11	$0.08	$0.14	$0.21
	Stainless Steel*	$3.97	$3.97	$3.97	$3.97	0.375	0.65	0.25	$0.24	$0.24	$0.24	$0.24
	SS-CCC	$2.60	$2.60	$2.60	$2.60	0.375	0.65	0.25	$0.16	$0.16	$0.16	$0.16

*Costs for these bar types were calculated in the final report for R27-SP49 (Gombeda et al., 2022).

^Does not incorporate the modified high-strength reinforcement factor in this case, as this factor is now cross-section dependent. These results must be multiplied by the modified high-strength reinforcement factor to determine complete life-cycle costs in this updated framework. A set of simple examples is provided in the appendix of this report.

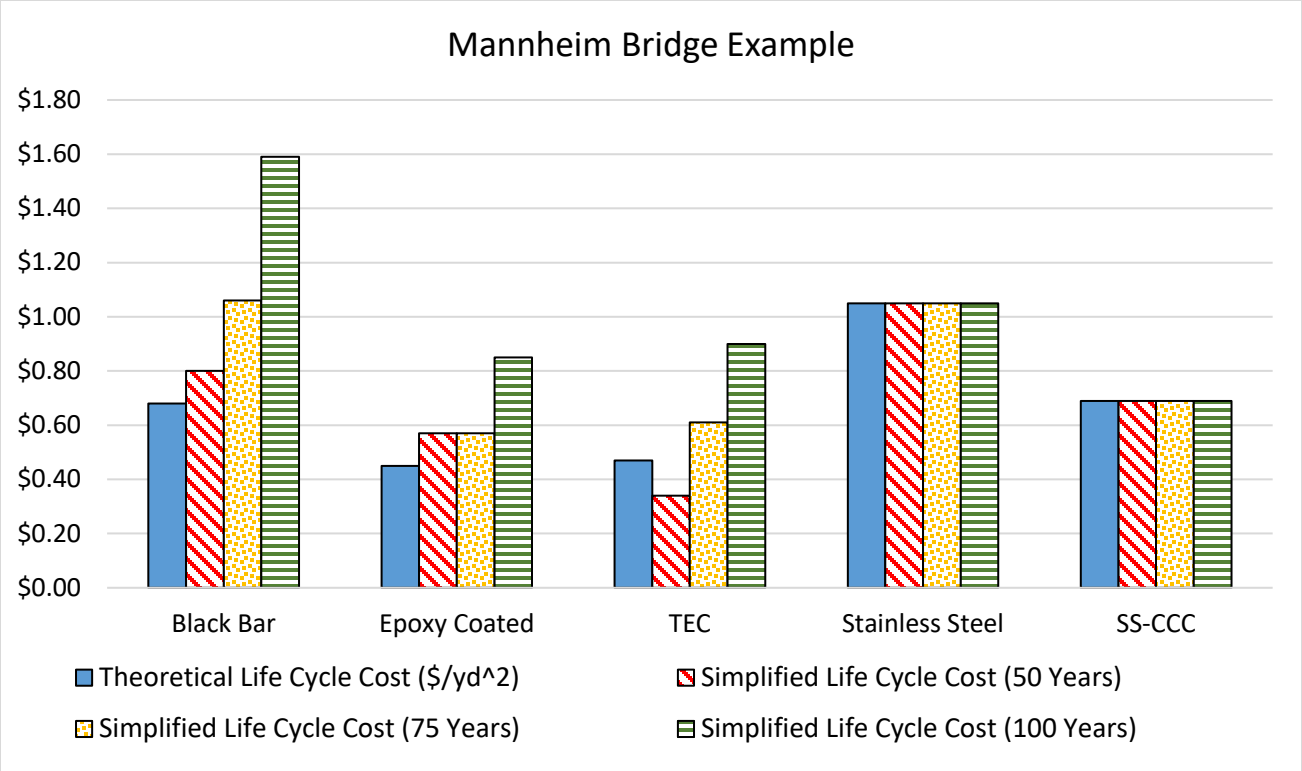

Figure 14. Graph. Graphical representation of life-cycle cost estimates for the first example.

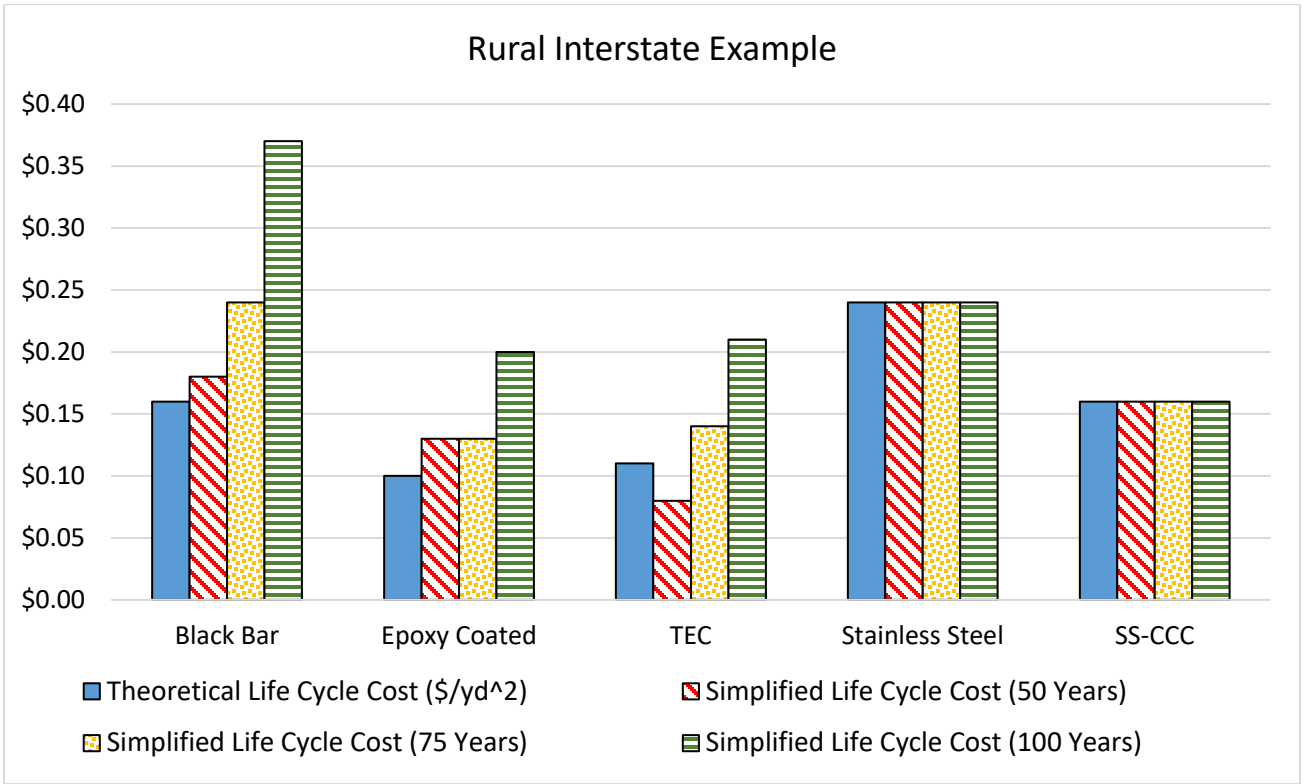

Figure 15. Graph. Graphical representation of life-cycle cost estimates for the second example.

CHAPTER 5: SUMMARY AND CONCLUSIONS

This study was the second phase of the Illinois Center for Transportation and Illinois Department of Transportation project R27-SP49. This project aimed to holistically determine the optimal reinforcement type that facilitates the desired balance between enhanced corrosion resistance and estimated life-cycle costs. This follow-up study focused on three distinct components. The first and second components examined life-cycle cost implications when using textured epoxy-coated and stainless steel–clad carbon core bars, respectively, in a slightly revised version of the original framework. The third component involved developing a more robust approach for assessing the combined effects of the higher yield strength and corresponding reduction in ductility for A1035 bars. Comprehensive literature reviews were conducted for both TEC and SS-CCC bars in Chapter 2 of this report and a detailed numerical study was used in Chapter 3 to develop a new, modified high-strength reinforcement factor for use in the updated life-cycle cost framework. The outcomes from these efforts were then used to estimate life-cycle costs for each new bar option (i.e., TEC and SS-CCC) followed by assessing the effectiveness of these bars using two hypothetical bridge deck examples. As demonstrated in R27-SP49, enhanced corrosion performance often comes with a significant trade-off of higher initial material costs, which for some applications may restrict the use of higher performance corrosion-resistant bar options—especially in the absence of running a detailed life-cycle cost analysis. The outcomes of this study further highlight the importance of considering life-cycle costs, as reinforcement options with higher initial costs often facilitate reduced overall life-cycle costs due to reduced (or even mitigated in some cases) maintenance events over a 100-year design service life. This conclusion is especially true for SS-CCC bars, which generally exhibit similar corrosion performance but have relatively lower upfront material costs similar to that of traditional stainless-steel bars—even though the initial price point is approximately double that of conventional black bars or regular epoxy-coated bars.

More specifically, the following conclusions can be drawn based on the outcomes of this study:

1. Textured epoxy-coated bars are relatively similar to regular epoxy-coated bars in initial costs and performance over a design 100-year life cycle, with the textured bars having very slightly higher upfront costs and slightly longer durations between recommended maintenance events. A primary motivator for using the textured bars, therefore, may be driven by more specific structural performance requirements, such as bond or development with the surrounding concrete. Further research is likely needed to fully assess life-cycle implications for these bars, as the data available as of the preparation of this report is relatively limited.

2. Despite being approximately one-half of the initial cost, stainless steel clad–carbon core bars exhibit a very similar maintenance cycle as the solid stainless-steel bars. This performance is largely due to the stainless-steel cladding, which provides enhanced corrosion resistance at the surface of the bar while optimizing material costs with a more economical carbon steel core that is effectively shielded from harmful deterioration agents. Additionally, the cladding is fused to the underlying carbon core during rolling, which provides enhanced structural integrity of the cladding itself when compared to

epoxy-coated bars, which often require special precautions to mitigate damage to the more fragile coating. The life-cycle costs for SS-CCC bars are lower than standard black bars, both regular and textured epoxy-coated bars, and traditional stainless-steel bars at longer design service lives.

3. Despite the higher nominal yield strength, A1035 reinforcing steel exhibits significantly reduced ductility when compared to conventional Grade 60 reinforcing steels. As an improvement to the simple nominal yield strength factor originally proposed as part of R27-SP49, a modified high-strength reinforcement factor was developed in this study. The reduced ductility, and its corresponding effect on the design of concrete bridge decks with A1035 bars, was captured herein by assessing the difference between the net tensile strain and the yield strain of the material—both computed during the design process—relative to the corresponding net tensile and yield strains of an equivalent cross-section containing conventional Grade 60 bars. The resulting modified high-strength reinforcement factor, ψ, is therefore able to capture the combined effects of reinforcement over-strength (i.e., the actual remaining moment resistance past the nominal flexural resistance) and relative ductility at the nominal flexural resistance. After a concise parametric study, it was concluded that the new factor was able to distinguish cross-sections with reduced ductility and therefore induce a more informed, albeit more stringent reduction on overall life-cycle costs. Moreover, life-cycle cost savings may be slightly less when using the modified high-strength reinforcement factor relative to the older approach that utilized the simpler nominal yield strength factor in project R27-SP49—but is expected to correspond to enhanced reliability due to the new considerations for ductility performance.

REFERENCES

American Association of State and Highway Transportation Officials. (2019). *AASHTO M 329M/M 329-11 standard specification for stainless clad deformed and plain round steel bars for concrete reinforcement*. AASHTO.

Andrawes, B., Perez Claros, E., & Zhang, Z. (2022). *Bond characteristics and experimental behavior of textured epoxy-coated rebars used in concrete bridge decks* (Report No. FHWA-ICT-22-001). Illinois Center for Transportation. https://doi.org/10.36501/0197-9191/22-001

ASTM International. (2019). *ASTM A959-19 standard guide for specifying harmonized standard grade compositions for wrought stainless steels*. ASTM International. https://www.astm.org/a0959-19.html

ASTM International. (2020). *ASTM A1035 specification for deformed and plain, low-carbon, chromium, steel bars for concrete reinforcement*. ASTM International.

ASTM International. (2019). *ASTM A264-12 standard specification for stainless chromium-nickel steel-clad plate*. Accessed February 7, 2023. https://www.astm.org/a0264-12r19.html

Clemeña, G. G., Kukreja, D. N., & Napier, C. S. (2003). *Trial use of a stainless steel-clad steel bar in a new concrete bridge deck in Virginia* (Report No. FHWA/VTRC 04-R5). Virginia Transportation Research Council.

Gombeda, M. J., Naito, C. J., & Quiel, S. E. (2019). Visual damage at flexural response milestones for blast-resistant precast concrete panels with varying reinforcement. *Engineering Structures*, *189* (November 2018), 174–185. https://doi.org/10.1016/j.engstruct.2019.03.014

Gombeda, M. J., Trasborg, P. Naito, C. J., & Quiel, S. E. (2017). Simplified model for partially-composite precast concrete insulated wall panels subjected to lateral loading. *Engineering Structures*, *138*(1), 367–380. https://doi.org/10.1016/j.engstruct.2017.01.065

Gombeda, M., Rivera, E., & Lallas, Z. (2022). *Optimal approach for addressing reinforcement corrosion for concrete bridge decks in Illinois* (Report No. FHWA-ICT-22-005). Illinois Center for Transportation. https://doi.org/10.36501/0197-9191/22-005

Illinois Department of Transportation. (2012). *Bridge Manual*. Bureau of Bridges and Structures, Division of Highways, Illinois Department of Transportation.

Kahl, S. (2012). *Stainless and stainless-clad reinforcement for highway bridge use* (Report No. RC-1560). Minnesota Transportation Commission.

Kim, K.-H. E., & Andrawes, B. (2018). *Behavior of epoxy-coated textured reinforcing bars* (Report No. FHWA-ICT-18-004). Illinois Center for Transportation. https://doi.org/10.36501/0197-9191/18-005

Murphy, Aaron J., "Comparison of Flexural Cracking in Reinforced Concrete Beams with Different Rebar Coatings" (2021). Clemson university. All Theses. 3535.

NX Infrastructure. (2018) “NX Stainless Steel Clad Rebar.” https://www.nxinfrastructure.com/nx-stainless-steel-clad-rebar

Peterman, R. J. (2009). A simple quality assurance test for strand bond. *PCI Journal*, *54*(2), 143–161.

https://doi.org/10.15554/pcij.03012009.143.161

Ross, B., Poursaee, A., Sreedhara, S., Mueller, M. (2021). Textured epoxy-coated and Galvanized Reinforcement to Reduce Cracking in Concrete Bridge Decks and Components. WisDOT ID no. 0092-19-01.

Tanks, J. D., & Sharp, S. R. (2015). Characterization of a stainless-clad steel reinforcing bar. *TRB 94th Annual Meeting Compendium of Papers*.

APPENDIX: SAMPLE CALCULATIONS

EXAMPLE—COMPARISON OF UPDATED THEORETICAL AND SIMPLIFIED LIFE-CYCLE COSTS BASED ON CROSS SECTION

Determination of reinforcement sizing, and thus the ductility and high-strength reinforcement factors (λ and ψ, respectively), was calculated based on equilibrating nominal flexural resistance of the sections. Thus, the reinforcement sizing in each condition below can be approximated as equivalent for the purposes of flexural resistance.

For the purposes of this example, only A1035 reinforcement is considered since types of Grade 60 reinforcement are unaffected by the high-strength reinforcement factor. Additionally, this example will only contain section S8.5t7.5. For the purposes of this example, only one location is outlined. The location selected was Mannheim Bridge (Lake and St. Charles), Cook County.

NOTE: The following procedure shows the conversion starting with the original NYSF to the modified high-strength reinforcement factor. The NYSF need not be used at all if calculating life-cycle costs using solely the modified procedure outlined in this report (i.e., simply multiply the expanded material life-cycle cost by the high-strength reinforcement factor, ψ, and corresponding WF, SF, and AADT factors). Notation: ε_y is the reinforcement strain at first yield and ε_t is the net tensile strain.

Negative Moment

A1035 (80% of Nominal Yield Strength) – S8.5t7.5

Design ε_y (in/in): 0.00276
Design ε_T (in/in): 0.00866
Ductility Factor, λ: 0.916
High-Strength Reinforcement Factor, ψ: 0.819

(The following values were taken from Project R27-SP49 Report.)
Nominal Yield Strength Factor (NYSF): 0.75
ψ/NYSF: 1.092
[Expanded] Theoretical Material Life-Cycle Cost ($/0.84m^2) [$/yd^2]: $0.30
Simplified Life-Cycle Cost:

- 50 & 75 Years: $0.38
- 100 Years: $0.55

$$Updated\ Life\ Cycle\ Cost = Life\ Cycle\ Cost \times \frac{\psi}{NYSF}$$

$$Updated\ Theoretical\ Material\ Life\ Cycle\ Cost = \$0.30 \times 1.092 = \$0.33$$

	Simplified Life Cycle Cost (LCC)	*Updated Simplified LCC*
Theoretical Mat. LCC	*$0.30*	*$0.33*
50 & 75 Years	*$0.38*	*$0.41*
100 Years	*$0.55*	*$0.60*

A1035 (100% of Nominal Yield Strength) – S8.5t7.5
Design ε_y (in/in): 0.00345
Design ε_T (in/in): 0.00875
Ductility Factor, λ: 0.824
High-Strength Reinforcement Factor, ψ: 0.729

(The following values were taken from Project R27-SP49 Report.)
Nominal Yield Strength Factor (NYSF): 0.6
ψ/NYSF: 1.214
[Expanded] Theoretical Material Life-Cycle Cost ($/0.84m^2) [$/yd^2]: $0.30
Simplified Life-Cycle Cost:

- 50 & 75 Years: $0.38
- 100 Years: $0.55

$$Updated\ Theoretical\ Material\ Life\ Cycle\ Cost = \$0.30 \times 1.214 = \$0.36$$

	Simplified Life Cycle Cost (LCC)	*Updated Simplified LCC*
Theoretical Mat. LCC	*$0.30*	*$0.36*
50 & 75 Years	*$0.38*	*$0.46*
100 Years	*$0.55*	*$0.67*

<u>Positive Moment</u>
A1035 (80% of Nominal Yield Strength) – S8.5t7.5
Design ε_y (in/in): 0.00276
Design ε_T (in/in): 0.00880
Ductility Factor, λ: 0.938
High-Strength Reinforcement Factor, ψ: 0.800

(The following values were taken from Project R27-SP49 Report.)
Nominal Yield Strength Factor (NYSF): 0.75
ψ/NYSF: 1.066
[Expanded] Theoretical Material Life-Cycle Cost ($/0.84m^2) [$/yd^2]: $0.30
Simplified Life-Cycle Cost:

- 50 & 75 Years: $0.38
- 100 Years: $0.55

$$Updated\ Theoretical\ Material\ Life\ Cycle\ Cost = \$0.30 \times 1.066 = \$0.32$$

	Simplified Life Cycle Cost (LCC)	*Updated Simplified LCC*
Theoretical Mat. LCC	*$0.30*	*$0.32*
50 &75 Years	*$0.38*	*$0.41*
100 Years	*$0.55*	*$0.59*

A1035 (100% of Nominal Yield Strength) – S8.5t7.5
Design ε_y (in/in): 0.00345
Design ε_T (in/in): 0.00928
Ductility Factor, λ: 0.906
High-Strength Reinforcement Factor, ψ: 0.662

(The following values were taken from Project R27-SP49 Report.)
Nominal Yield Strength Factor (NYSF): 0.6
ψ/NYSF: 1.104
[Expanded] Theoretical Material Life-Cycle Cost ($/0.84m^2) [$/yd^2]: $0.30
Simplified Life-Cycle Cost:

- 50 & 75 Years: $0.38
- 100 Years: $0.55

$$Updated\ Theoretical\ Material\ Life\ Cycle\ Cost = \$0.30 \times 1.104 = \$0.33$$

	Simplified Life Cycle Cost (LCC)	*Updated Simplified LCC*
Theoretical Mat. LCC	*$0.30*	*$0.33*
50 & 75 Years	*$0.38*	*$0.42*
100 Years	*$0.55*	*$0.61*


Illinois Department
of Transportation


ILLINOIS